Coupling carboxylic acid reductase to inorganic pyrophosphatase enhances cell-free in vitro aldehyde biosynthesis

Citation: Kunjapur, Aditya M., Bernardo Cervantes, and Kristala L. J. Prather. "Coupling Carboxylic Acid Reductase to Inorganic Pyrophosphatase Enhances Cell-Free in Vitro Aldehyde Biosynthesis." Biochemical Engineering Journal 109 (2016): 19-27.

As Published: 10.1016/J.BEJ.2015.12.018

Publisher: Elsevier BV

Persistent URL: https://hdl.handle.net/1721.1/134475

Version: Author's final manuscript: final author's manuscript post peer review, without publisher's formatting or copy editing

Title: Coupling carboxylic acid reductase to inorganic pyrophosphatase enhances cell-free *in vitro* aldehyde biosynthesis

Authors: Aditya M. Kunjapur[1,2,3], Bernardo Cervantes[4], Kristala L. J. Prather[1,2,4]*

Affiliations:

1. Department of Chemical Engineering, Massachusetts Institute of Technology, Cambridge, MA 02139, USA
2. Synthetic Biology Engineering Research Center (SynBERC), Massachusetts Institute of Technology, Cambridge, MA 02139, USA
3. Present Address: Department of Genetics, Harvard Medical School, Boston, MA 02115, USA
4. Microbiology Graduate Program, Massachusetts Institute of Technology, Cambridge, MA 02139, USA

* Corresponding author:

Department of Chemical Engineering

77 Massachusetts Avenue

Room E17-504G

Cambridge, MA 02139

Phone: 617.253.1950

Fax: 617.258.5042

Email: kljp@mit.edu

Keywords: aldehydes, carboxylic acid reductase, biocatalysis, enzyme biocatalysis, modelling, production kinetics

Abstract:

Carboxylic acid reductases (CARs) have been harnessed in metabolic pathways to produce aldehydes in engineered organisms. However, desired aldehyde products inhibit cell growth and limit product titers currently achievable from fermentative processes. Aldehyde toxicity can be entirely circumvented by performing aldehyde biosynthesis in non-cellular systems. Use of purified CARs for preparative-scale aldehyde synthesis has been limited by *in vitro* turnover of model CARs, such as Car_{Ni} from *Nocardia iowensis*, despite robust conversion of substrates associated with expression in heterologous hosts such as *E. coli* and yeast. In this study, we report that *in vitro* activity of Car_{Ni} is inhibited by formation of the co-product pyrophosphate, and that pairing of an inorganic pyrophosphatase (Ppa_{Ec}) with Car_{Ni} substantially improves the rate and yield of aldehyde biosynthesis. We demonstrate that, in the presence of Ppa_{Ec}, Michaelis-Menten kinetic models based on initial rate measurements accurately predict Car_{Ni} kinetics within an *in vitro* pathway over longer timescales. We rationalize our novel observations for Car_{Ni} in part using previously posed thermodynamic arguments for ATP hydrolysis, and we compare our results with those observed for other adenylate-forming enzymes. Overall, our findings may aid in increasing adoption of CARs for cell-free *in vitro* aldehyde biosynthetic processes.

Main Text:

1 Introduction

Aldehydes find uses in many industries, including the flavors and fragrances industries. Vanillin and benzaldehyde, which are two aromatic aldehydes that respectively provide vanilla and almond flavors, are the two flavor additives to food products with the largest global annual markets by quantity [1-3]. Other aldehydes with relevance to the flavor industry are aliphatic (fatty) aldehydes such as hexanal, octanal, decanal, and dodecanal, as well as terpenoid aldehydes such as citral and safranal [4-6]. Plant extracts that naturally contain desired aldehydes for flavor applications are often expensive and/or scarce, most notably in the cases of vanillin and safranal [6, 7]. However, in the flavor industry and other industries requiring high purity, additives that are produced biologically without the use of harsh chemicals or severe processing conditions are often considered "natural" from a regulatory perspective and may be priced commensurate with their plant-derived counterparts [8]. If markets are sufficiently large, such molecules may represent more attractive targets than commodity chemicals for the development of biotechnological production processes.

Two broad classes of bioprocesses are capable of generating aldehydes from more abundant and affordable natural precursors: (i) whole-cell microbial conversion processes; or, (ii) cell-free conversion processes [9, 10]. Advantages of using microbial conversion include the ability to use less expensive inputs and more easily achieve economies of scale through large fermentations. However, cell-based aldehyde synthesis processes are limited by the rapid reduction of aldehydes to alcohols by endogenous reductases [11, 12] and by toxicity to the host cell [12-15]. Aldehyde reduction can be minimized by deleting genes encoding endogenous reductases [12]; however, mitigation of toxicity effects remain unsolved. Cell-free or *in vitro* biosynthetic

routes could be used to circumvent both the aldehyde stability and toxicity issues, with the minor exception of aldehyde adducts that may form on, and inhibit, aldehyde biosynthetic enzymes.

In recent years, carboxylic acid reductases (CARs) have shown outstanding promise for their use in aldehyde biosynthesis [11, 16]. The carboxylic acid reductase from *Nocardia iowensis* (Car_{Ni}) is a model CAR that has been characterized *in vitro*, was found to be active on diverse aldehyde substrates ranging across aromatic and aliphatic families, and has been expressed in *E. coli* and *S. cerevisiae* to enable microbial production of aldehydes from carboxylic acid precursors that are supplied exogenously to cultures or produced intrinsically from metabolism [12, 17-22]. Many of the carboxylic acid precursors can be found more inexpensively in nature than their corresponding desired aldehyde. Carboxylic acids can also serve as the target for microbial production with minimal toxicity, and subsequently, the carboxylic acid product from fermentation can be separated and converted to aldehyde in a cell-free environment. The first report detailing the biosynthesis of vanillin from glucose harnessed such a two stage approach [23]. Like other soluble enzymes, CARs can also be utilized in the three main types of cell-free systems: they can be expressed in cells that are later lysed to generate cell-extracts (CFX); they can be synthesized *in vitro* using dilute aqueous systems that contain transcription (TX) and translation (TL) machinery for cell-free protein synthesis (CF TX-TL or CFPS) [24]; or alternatively, they can be purified and added to dilute aqueous *in vitro* solutions [9, 10].

One primary obstacle to the use of purified CARs for cell-free *in vitro* aldehyde biosynthesis is their low conversion of carboxylic acids in dilute systems [18, 25]. In this report, we investigate why CARs are subject to apparently limited turnover *in vitro* using the model CAR from *Nocardia iowensis* (Car_{Ni}). We identify that a known co-product of the reaction, pyrophosphate (PP_i), is inhibitory. Addition of inorganic pyrophosphatase sourced from *E. coli*

substantially improves turnover, enabling predictable pathway kinetics using simple Michaelis-Menten models and improving final conversion nearly two-fold under some of the conditions investigated.

2 Materials and Methods

2.1 Plasmid construction

Escherichia coli DH10B (Invitrogen, Carlsbad, CA) was used for plasmid cloning transformations and plasmid propagation. PCR amplification was performed using custom oligonucleotides (Sigma-Genosys, St. Louis, MO) (**Table 1**) and Q5 High-Fidelity DNA polymerase (New England Biolabs, Ipswich, MA). Restriction enzymes were obtained from New England Biolabs. In order to potentially study the effect of enzyme co-localization in a subsequent study, C-terminal peptide tags corresponding to synthetic protein scaffold domains appended to flexible glycine-serine linkers were added to Car_{Ni} and to $YtbE_{Bs}$ prior to expression and purification. In addition, N-terminal hexahistidine (His) tags were added to enable nickel-affinity purification. As previously described, the codon-optimized gene encoding Car_{Ni} was first cloned to generate the pET/His-Car-RBS2-Sfp vector [12, 22]. Next, the gene encoding Car_{Ni} was amplified by PCR using two sets of oligonucleotides (first "Car-GBD-f" and "Car-GBD-r1", and next "Car-GBD-f" and "Car-GBD-r2") in order to add a sequence encoding the GBD domain cognate peptide to the open reading frame [26]. This amplicon was then cloned into the same site as the original Car_{Ni} using the restriction enzymes BamHI and NotI. The untagged version of Car_{Ni}, which we purified and assayed previously [22], has very similar activity and is subject to the same limited turnover phenomenon. The gene encoding $YtbE_{Bs}$ was amplified from *Bacillus subtilis* PY79 genomic DNA (gDNA) by PCR and then cloned into the pCDFDuet vector (Novagen, Madison, WI) using the restriction enzymes BamHI and SalI. Next, the gene encoding $YtbE_{Bs}$ was

amplified by PCR in order to add a sequence encoding the SH3 domain cognate peptide to the open reading frame [26]. This amplicon was then cloned into the same site as the original $YtbE_{Bs}$ using the restriction enzymes BamHI and SalI. The gene encoding Ppa_{Ec} was amplified from *E. coli* MG1655 gDNA and cloned into the pTEV5 vector using the restriction enzymes NdeI and NotI. *B. subtilis* and *E. coli* gDNA were prepared using the Wizard Genomic DNA purification kit (Promega, Madison, WI).

Table 1. Oligonucleotides used in this study.

Name	Sequence (5' → 3')
Car-GBD-f	CATCACCATCATCACCAC
Car-GBD-r1	GTGGATGGCTCTGCTTCTCTTCTGCATCACGTGCATCAGGGCACCCACCA GTCCAGAGCCACTACCGTTGCAGCAGTTCCA
Car-GBD-r2	AAAAAAGCGGCCGCTCAATCTTCATCTTCATCGCCAGCCTGGTCCTCCCC TTCGTCGGAGGAGTGGATGGCTCTGCT
YtbE-f	AAAAAAGGATCCAATGACAACACATTTACAAG
YtbE-r	AAAAAAGTCGACATTAAAAATCAAAGTTGTC
YtbE-SH3-f	CTTTAATAAGGAGATATACCAT
YtbE-SH3-r	TTTTTTGTCGACTCACCCCGGACGGCGACGTTTTGGCGGAAGAGCTGGCG GAGGGCCAGAACCGCTACCGAAATCAAAGTTGTCCG
Ppa-f	AAAAAACATATGAGCTTACTCAACGTCCCT
Ppa-r	AAAAAAGCGGCCGCTTATTTATTCTTTGCGCGCT

2.2 Chemicals

Commercial inorganic pyrophosphatase (sourced from *E. coli*) was purchased from New England Biolabs. The following compounds were purchased from Sigma: benzoic acid, benzaldehyde, benzyl alcohol, vanillic acid, vanillin, magnesium chloride, dithiothreitol (DTT), ATP disodium salt hydrate, AMP disodium salt, NADPH tetrasodium salt, $NADP^+$ sodium salt, and sodium pyrophosphate tetrabasic. Isopropyl β-D-1-thiogalactopyranoside (IPTG) was

purchased from Denville Scientific. Ampicillin sodium salt and streptomycin sulfate were purchased from Affymetrix.

2.3 Enzyme purification

All proteins in this study were overproduced using *Escherichia coli* BL21 Star (DE3) obtained from Invitrogen. All proteins were purified using two-step purification techniques to ensure high purity. SDS-PAGE gels of purified proteins are presented in Fig. S1. Car_{Ni} and $YtbE_{Bs}$ were purified using sequential affinity and anion exchange chromatography. An overnight culture harboring either pET/His-Car-GBDtag-RBS2-Sfp or pCDF/His-YtbE-SH3tag was used as 10% (v/v) inoculum in two liters of LB Broth containing either 100 mg/L ampicillin or 50 mg/L streptomycin, respectively. Cultures were incubated at 30°C and 250 rpm, and expression was induced using a final concentration of 1 mM IPTG at an OD_{600} of 0.6. Cells were harvested after 20 hours using centrifugation and resuspended in Buffer A (100 mM MOPS-NaOH [pH 7.0], 300 mM NaCl, and 10% glycerol). Cells were subsequently lysed using sonication. The supernatant was collected, supplemented with imidazole (5 mM) and batch bound at 4°C for 2 h to 1 mL of Ni-NTA resin (Qiagen, Germantown, MD). The resin was washed with Buffer A containing 7.5 mM imidazole and subsequently poured into a column. Affinity chromatography was performed using step-wise increasing concentrations of imidazole (20, 40, 60, 100, and 250 mM). Fractions containing purified His-tagged enzyme were pooled and dialyzed overnight at 4°C into Buffer B (100 mM MOPS-NaOH [pH 7.0], 50 mM NaCl, 1 mM DTT, and 10% glycerol).

For subsequent anion exchange chromatography, dialyzed fractions were loaded onto a 5x5 mL HiTrap Q HP anion exchange column (GE Life Sciences, Piscataway, NJ) via a superloop, which were integrated into an ÄKTApurifier with a UNICORN control system v5.20 and a Frac-950 collector (GE Life Sciences). The purification was performed at a flow rate of 1 ml/minute at

4 °C. An initial wash of 25 ml was followed by a linear gradient from 50 mM NaCl to 500 mM NaCl for 100 ml elution volume. Fractions of 2 ml were collected and absorbance at 280 nm was used to determine desired fractions. Desired fractions were pooled and dialyzed once again in Buffer B to reduce salt content. Dialyzed enzyme was then flash frozen using liquid nitrogen and stored at -80°C.

The gene encoding Ppa_{Ec} was inserted into the pTEV5 vector for protein purification, leading to an enzyme product containing a His tag removable by treatment with TEV protease. One liter of cells harboring pTEV5/Ppa was grown at 30°C and 250 rpm in LB medium containing 100 mg/liter of ampicillin. Expression was induced using a final concentration of 1 mM IPTG at an OD_{600} of 0.6. Cells were harvested after 20 hours using centrifugation and resuspended in Buffer A. Cells were subsequently lysed using sonication. The supernatant was collected, supplemented with imidazole (5 mM) and batch bound at 4°C for 2 h to 1 mL of Ni-NTA resin (Qiagen, Germantown, MD). The resin was washed with Buffer A containing 7.5 mM imidazole and subsequently poured into a column. Affinity chromatography was performed using step-wise increasing concentrations of imidazole (20, 40, 60, 100, and 250 mM). Fractions containing purified His-Ppa_{Ec} were pooled along with 0.5 mg His-tagged TEV protease and dialyzed overnight at 4°C into Buffer B. The dialyzed and TEV-digested protein was passed through 1 ml of Ni-NTA resin to remove His-Ppa_{Ec} and His-tagged TEV protease. The untagged Ppa_{Ec} that did not bind to the resin was collected, flash frozen using liquid nitrogen, and stored at -80°C. Qualitative purity of all protein fractions were determined using SDS-PAGE (Bio-Rad, Hercules, CA). All protein concentrations were determined using the Bradford assay with bovine serum albumin as a standard [27].

2.4 Kinetic studies

Michaelis-Menten parameters for Car_{Ni} on benzoate were determined by measuring changes in absorbance at 340 nm for up to 5 minutes. Reactions were prepared as follows: 100 mM MOPS-NaOH [pH 7.0], 10 mM $MgCl_2$, 0.6 mM NADPH, 1 mM ATP, 224 nM Car_{Ni}, and at 6 different concentrations of pH neutralized benzoic acid. All concentrations were assayed in triplicate. MOPS was used instead of Tris to buffer our reactions given the propensity of Tris to react with aldehydes [28, 29]. MATLAB R2013a (Mathworks) was used to calculate kinetic parameters and model *in vitro* pathway kinetics.

Michaelis-Menten parameters for $YtbE_{Bs}$ on benzaldehyde were determined by measuring changes in absorbance at 340 nm for up to 5 minutes. Reactions were prepared as follows: 100 mM MOPS-NaOH [pH 7.0], 10 mM $MgCl_2$, 0.6 mM NADPH, 1 mM ATP, 1422 nM $YtbE_{Bs}$, and at 6 different concentrations of benzaldehyde. All concentrations were assayed in triplicate.

For all *in vitro* experiments excluding initial rate measurements, samples were quenched using 1% TFA and then subject to centrifugation. Aqueous supernatant was collected for HPLC analysis using either an Agilent 1100 series or 1200 series instrument equipped with a diode array detector. Wavelengths of 223, 242, and 192 nanometers were used to detect benzoic acid, benzaldehyde, and benzyl alcohol, respectively. The benzoate family of analytes was separated using an Aminex HPX-87H anion-exchange column (Bio-Rad Laboratories), with a mobile phase consisting of 70% 5 mM H_2SO_4 and 30% acetonitrile. All three compounds eluted within 35 minutes at a flow rate of 0.4 ml/min. Column temperature was maintained at 30°C. All chemicals reported in figures were quantified using calibration of standards on the HPLC instrument and linear interpolation. All experiments were performed in duplicate. Data points shown are averages with error bars calculated using the following formula, which is ordinarily used to determine

standard deviation but which does not result in a value with the same statistical power in this case given only duplicate measurements:

$$s = \sqrt{\frac{\sum_{i=1}^{n}(x_i - \bar{x})^2}{n-1}}$$

Conversion of vanillate to vanillin was determined using a Zorbax Eclipse XDB-C18 column (Agilent) and detected using a wavelength of 280 nm. A gradient method used the following solvents: (A) 50% acetonitrile + 0.1% trifluoroacetic acid (TFA); (B) water + 0.1% TFA. The gradient began with 5% Solvent A and 95% Solvent B. The setting at 20 minutes was 60% Solvent A and 40% Solvent B. The program restored the original ratio at 22 minutes and ended at 25 minutes. The flow rate was 1.0 ml/min and all compounds of interest eluted within 15 minutes. Column temperature was maintained at 30°C.

3 Results

3.1 Pyrophosphatase addition improves *in vitro* Car$_{Ni}$-catalyzed conversion

The overall reaction catalyzed by Car$_{Ni}$ proceeds via several steps that require components beyond the carboxylic acid substrate and Car$_{Ni}$ apoenzyme [19]. A phosphopantetheinyl transferase must attach a phosphopantetheine group to Car$_{Ni}$ in order to form an activated holoenzyme. Car$_{Ni}$ catalyzes the ATP-dependent and Mg^{2+}-dependent formation of an acyl-adenylate (or acyl-AMP) intermediate at its N-terminal adenylating domain. The Mg^{2+} ion is reported to neutralize the charge of ATP, stabilize the transition state, and neutralize the leaving phosphate [30]. The thiol group belonging to the phosphopantetheine arm of activated Car$_{Ni}$ subsequently binds to the acyl group, resulting in a covalently bound acyl-enzyme intermediate and the release of AMP. Once the phosphopantetheine arm “swings” to the C-terminal reductase

domain, the NADPH-dependent reduction of the acyl group into a released aldehyde occurs. After reactivation of the thiol group, a new catalytic cycle follows [19]. The simplified net reaction catalyzed by Car_{Ni} for the model substrate benzoate is depicted in **Fig. 1A**.

When initially performing *in vitro* experiments with Car_{Ni} and required co-factors in dilute buffered solution, we observed a steady decline in reaction rate and gradual formation of a precipitate. Given the possibility that precipitation may be contributing to the decline in Car_{Ni} activity, we sought to determine the minimal set of components responsible for precipitation. Upon mixing all possible pairs of substrates, products, and co-factors (benzoate, $MgCl_2$, ATP, NADPH, benzaldehyde, AMP, PP_i, and $NADP^+$) in separate solutions, we found that only $MgCl_2$ and PP_i were forming precipitate. Interestingly, it is known that $MgCl_2$ and PP_i form a precipitate, whereas $MgCl_2$ and orthophosphate do not [31]. To better understand the possible influence of precipitation on the reaction catalyzed by Car_{Ni}, we explored two questions. One question was whether an increase in the initial concentration of $MgCl_2$ in assay solutions would increase soluble Mg^{2+} available for the reaction and thereby extend the number of turnovers. A second question was whether precipitate formation could be minimized by breakdown of PP_i. To accomplish the latter, we added commercial inorganic pyrophosphatase from *E. coli* (Ppa_{Ec}) to our assay solution, which catalyzes the conversion of PP_i to inorganic phosphate (**Fig. 1B**). Benzoate consumption increased after both perturbations, albeit more substantially with the breakdown of PP_i (**Fig. S2**). Precipitation was not observed in samples containing commercial Ppa_{Ec}.

To investigate the possible effects of Mg^{2+} concentration and pyrophosphatase addition more thoroughly, we began by overexpressing and purifying the inorganic pyrophosphatase from *E. coli* in order to exclude the possibility that another component from the commercial Ppa_{Ec} mixture was influencing observed enhancement. In addition, given our curiosity about possible

alternatives that may shift equilibrium, we compared three modified assay conditions against a control assay (**Fig. 1C**). All assays contained 1 mM benzoate, 6 mM NADPH, and 224 nM Car_{Ni} added at the time of 0 mins, after all other components. The control also contained 6 mM ATP and 20 mM $MgCl_2$. The following deviations from the control were investigated: (i) 12 mM ATP; (ii) 12 mM ATP and 100 mM $MgCl_2$; (iii) 224 nM Ppa_{Ec}. Within each of the experimental groups, the concentrations of benzaldehyde product observed at 30 mins and 60 mins were similar. This result underscores the problem of limited turnovers, except in the case of Ppa_{Ec} addition, which led to nearly complete conversion of benzoate within 30 mins. Precipitate was observed in all samples except those containing Ppa_{Ec}. The other perturbations of increasing ATP concentration two-fold and Mg^{2+} concentration five-fold did not improve benzaldehyde synthesis. In fact, contrary to our previous experiment (**Fig. S2**), the increase in Mg^{2+} appeared to decrease the rate of benzoate conversion while maintaining a similar "final" benzoate conversion achieved by 60 mins.

3.2 Pyrophosphatase addition improves performance of a two-enzyme *in vitro* pathway containing Car_{Ni}

Given the encouraging result observed for consumption of the co-product pyrophosphate, we sought to evaluate whether consumption of the aldehyde product might also drive the reaction further towards completion. To that end, we overexpressed and purified the heterologous aldo-keto reductase $YtbE_{Bs}$ using *E. coli* [32, 33]. $YtbE_{Bs}$ is known to catalyze the NADPH-dependent conversion of aromatic aldehydes and ketones into their corresponding alcohols, including conversion of benzaldehyde into benzyl alcohol [32]. Addition of both Car_{Ni} and $YtbE_{Bs}$ into assay solutions would be expected to establish a two-step *in vitro* pathway from benzoate to benzyl alcohol (**Fig. 2A**). Consistent with previous studies that characterized each enzyme separately, we determined that $YtbE_{Bs}$ has lower catalytic efficiency (k_{cat}/K_M) than Car_{Ni}. Therefore, we

established our *in vitro* pathway using 224 nM Car_{Ni} and 1422 nM $YtbE_{Bs}$ in order to roughly balance flux between the first and second reaction. In these experiments, the objective was to identify conditions that would maximize benzyl alcohol yield.

The resulting concentration profiles of benzoate, benzaldehyde, and benzyl alcohol from experiments containing the pathway demonstrated that adding a sink for benzaldehyde did not drive further conversion of benzoate (**Fig. 2B**). The result also suggests that benzaldehyde does not inhibit Car_{Ni}. Once again, Ppa_{Ec} addition enhanced benzoate conversion as well as overall flux through the *in vitro* pathway (based on the final benzyl alcohol concentration) at the lower $MgCl_2$ concentration of 10 mM. However, Ppa_{Ec} addition did not improve flux through this pathway when 100 mM $MgCl_2$ was used. Previous studies have demonstrated that Ppa_{Ec} is Mg^{2+}-dependent and that activity saturates around concentrations of 10 mM Mg^{2+} [34, 35]. These reports do not document an inhibitory effect resulting from Mg^{2+} concentrations above 10 mM. Although we found that 100 mM $MgCl_2$ slightly reduced $YtbE_{Bs}$ activity (**Fig. S3)**, we do not expect the decrease in $YtbE_{Bs}$ activity to be solely responsible for the decrease in pathway flux. Given that higher Mg^{2+} concentrations did not seem to have a beneficial effect except in one initial experiment (**Fig. S2**), we used 10 mM $MgCl_2$ for all following experiments and did not investigate the role of Mg^{2+} in this system any further.

3.3 Pyrophosphatase addition improves predictability of Car_{Ni}-catalyzed *in vitro* reactions

We next sought to understand whether the enhancement observed by Ppa_{Ec} addition allowed reaction kinetics to be predictable based solely on initial rate measurements and simple Michaelis-Menten kinetic equations (see **Supplementary Text** for model formulation). If attainable, model predictability would be significant for its guiding insights on process design factors such as required enzyme concentration and reaction time for preparative-scale aldehyde

biosynthesis or for *in vitro* biosynthetic pathways to other products. We were first interested in simulating reactions containing only Car_{Ni}. To obtain model parameters, we performed initial rate measurements for Car_{Ni} with respect to benzoate (**Fig. 3A**), and we calculated the k_{cat} and K_M based on these data. Initial reaction rates for Car_{Ni} were no different within the first minute in the presence or absence of Ppa_{Ec}, indicating the challenge associated with obtaining a simple and relevant inhibition rate constant associated with gradual pyrophosphate formation and precipitation. Using an ODE solver in MATLAB, we plotted the analytical solutions for concentration profiles based on these parameters and initial substrate and enzyme concentrations (**Supplementary Text**). When Ppa_{Ec} is added to the reaction, we see that Car_{Ni}-catalyzed conversion of benzoate to benzaldehyde more closely achieves the simulated concentration one hour after addition of enzymes (**Fig. 3B**).

We were next interested in determining the simulated concentration profiles of a two-enzyme *in vitro* pathway containing Car_{Ni} and whether Ppa_{Ec} addition would more closely align observed results to simulated results. We performed initial rate measurements for $YtbE_{Bs}$ with respect to benzaldehyde (**Fig. 3C**) and subsequently tested the performance of the two-step *in vitro* pathway with and without addition of Ppa_{Ec} by measuring concentrations of benzoate, benzaldehyde, and benzyl alcohol at 0, 15, and 30 minutes after addition of enzymes (**Fig. 3D**). Observed pathway kinetics deviate from the model predictions within 15 minutes in the absence of Ppa_{Ec}. On the other hand, when Ppa_{Ec} is included in the system, pathway kinetics perform closely to model expectations for at least 30 minutes. Thus, Ppa_{Ec} addition not only improves Car_{Ni} conversion but enables more accurate kinetic modeling over longer timescales when Car_{Ni} is used *in vitro* individually or as part of a pathway.

3.4 More concentrated *in vitro* aldehyde biosynthetic reactions using Car_{Ni} display greater increases in conversion upon pyrophosphatase addition

Thus far, we had observed enhancement when starting with 1 mM benzoate, and we were curious to know whether Ppa_{Ec} addition would be as effective for higher initial substrate concentrations more characteristic of preparative-scale reactions. Furthermore, we wanted to learn whether enhancement from Ppa_{Ec} addition would quantitatively differ if an alternative substrate were used, especially given the promiscuity of Car_{Ni}. Our next experiment utilized 5 mM initial concentrations of benzoate or vanillate in the same single enzyme system as used originally, and we monitored substrate conversion with and without Ppa_{Ec} (**Fig. 4**). It is known that Car_{Ni} catalyzes the conversion of vanillate to vanillin more slowly than it catalyzes the conversion of benzoate to benzaldehyde [18]. The result from this experiment suggests that kinetic enhancement obtained by coupling Ppa_{Ec} to Car_{Ni} increases as substrate concentration increases (here roughly double the final conversion of benzoate and vanillate without Ppa_{Ec} addition) and occurs across different substrates.

3.5 Steps towards understanding why pyrophosphate hydrolysis enhances the reaction

To better understand the effects of PP_i hydrolysis on the reaction catalyzed by Car_{Ni}, we first explored the literature. Although reports featuring Car_{Ni} and its homologs have not discussed PP_i-related inhibition, PP_i has been identified as inhibitory for other adenylate-forming enzymes. In particular, *in vitro* transcription reactions catalyzed by RNA polymerase have been observed to form $Mg_2{\cdot}PP_i$, to be subject to limited turnover, and to be enhanced by addition of Ppa_{Ec} [36-38]. However, these studies offer differing perspectives on why PP_i may inhibit RNA polymerase. We examine these perspectives in more detail in the Discussion.

We performed two experiments to explore possible inhibitory roles of PP_i. First, we added exogenous sodium pyrophosphate to one of two otherwise identical reaction pairs at an initial concentration of 0.5 mM. After reactions incubated for one hour, we found that the reaction containing exogenous PP_i did not proceed as far (**Fig. S4A**). In addition, given our previous observations of precipitate and hypotheses offered in the literature for *in vitro* transcription [38], we briefly explored the possibility that there may be an interaction between Car_{Ni} and the precipitate (**Figs. S4B and S4C**). Based on SDS-PAGE results, we identified Car_{Ni} protein in the precipitate in the absence of Ppa addition. We also found increased Car_{Ni} in the precipitate when PP_i was generated by the reaction relative to when exogenous PP_i was supplied initially at the expected final concentration. However, the protein obtained in the precipitate represents roughly 1/100 of the total initial protein added and therefore this interaction contributes minimally to reaction termination.

4 Discussion

Cell-free biosynthetic processes are becoming relevant alternatives to fermentative processes for an increasing number of potential chemical products [39]. Furthermore, the cell-free research field aims to expand the range of attainable products by moving beyond single enzyme biocatalysis to construct metabolic pathways *in vitro*. Central to this aim is the ability to accurately model *in vitro* reaction kinetics for individual enzymes and for systems with greater complexity [40]. In this report, we have demonstrated that coupling Ppa_{Ec} to Car_{Ni} not only substantially improves conversion but enables accurate kinetic modeling for Car_{Ni} as part of a two enzyme pathway. *In vitro* aldehyde biosynthesis featuring Car_{Ni} is an excellent system for cell-free researchers and practitioners to build upon for several reasons. The promiscuity of Car_{Ni} and the reactivity of aldehydes may enable cell-free synthesis of a variety of aldehydes or aldehyde-

derived products upon addition of downstream enzymes [11]. In addition, aldehydes are a great class of chemicals for cell-free researchers to focus on given their cellular toxicity. As mentioned earlier, another benefit of cell-free processes specifically for aldehyde biosynthesis is that aldehydes will be rapidly converted to corresponding alcohols in cells or cell extract unless otherwise engineered [12].

Inorganic pyrophosphatases are abundant in living cells and are essential for growth of *E. coli* [35, 41-45]. Previously, they have been applied to PP_i-generating reactions for different purposes. In one application, pyrophosphatase forms part of a coupled enzyme kinetic assay with increased sensitivity because of the detection of inorganic phosphate as a proxy for product and the formation of two moles of inorganic phosphate for every one mole of PP_i [46]. In a manner analogous to its use here, pyrophosphatase has been used to enhance *in vitro* transcription reactions since the 1990s [47, 48]. In addition to increasing the yield of RNA synthesized, pyrophosphatase was also shown to minimize the effect of the Mg^{2+} concentration on product yields [47]. Interestingly, addition of pyrophosphatase increased synthesis of transcripts roughly twofold, and the lowest concentration of pyrophosphatase investigated provided full enhancement. These experimental observations for *in vitro* transcription are consistent with results reported in this study for pairing Ppa_{Ec} with Car_{Ni}.

There is disagreement in the literature about the mechanism by which PP_i inhibits the analogous, adenylate-forming *in vitro* transcription reaction catalyzed by RNA polymerase. A thermodynamic justification for why PP_i hydrolysis should improve the average degree of polymerization of RNA transcribed *in vitro* was documented as early as 1975 and is based on the irreversibility of hydrolysis, which should drive the adenylation reaction forward [36]. However, in 1997, Kern and Davis reported the application of solution equilibrium analysis to *in vitro*

transcription and concluded that the detrimental effect of PP_i on the reaction was primarily due to sequestering of magnesium as the $Mg_2{\cdot}PP_i$ gradually formed [37]. They observed that the reaction rate decreased substantially below 5 mM free Mg^{2+}. As recently as 2012, a detailed multiphysics modeling and experimental study further examined the effect of $Mg_2{\cdot}PP_i$ precipitation on *in vitro* transcription and offered yet another possibility [38]. These authors noted that previous studies had assumed that the $Mg_2{\cdot}PP_i$ precipitate forms immediately, whereas they demonstrated that the gradual formation of precipitate is consistent with a nucleation process that has an induction period. Importantly, they observed that transcription stops at the onset of precipitation but that the Mg^{2+} concentration does not decrease as much as expected by solution equilibrium [38]. Two possibilities were offered: (i) that an electrical double layer around the precipitate sequesters more Mg^{2+} than predicted by equilibrium analysis; or, (ii) that there may be a physical interaction between the $Mg_2{\cdot}PP_i$ precipitate and the RNA polymerase that inhibits the enzyme at the moment of transition even if the free Mg^{2+} concentration is sufficient [38]. They proposed that a single molecule assay may resolve the latter question in a future study. Based on our experimental observations for the reaction catalyzed by Car_{Ni}, we consider it unlikely that decreased free Mg^{2+} is a principal cause of reaction termination given the limited turnover we observed at higher $MgCl_2$ concentrations. Furthermore, while our precipitate analysis suggests there may be some physical interaction between Car_{Ni} and the $Mg_2{\cdot}PP_i$ precipitate, the amount of Car_{Ni} protein we found in the precipitate is not sufficient to be a principal cause of reaction termination.

When we discovered the history of pyrophosphatase use for *in vitro* transcription, we were curious to know whether pyrophosphatase addition might enhance all *in vitro* reactions featuring adenylate-forming enzymes, which universally generate PP_i as a co-product [30]. When we searched the literature for reports describing the effect of PP_i on other adenylate-forming enzymes,

we found that PP_i inhibits the fatty acid reductase complex from luminescent bacteria [49] and inhibits firefly luciferase *in vitro* [50]. However, we did not find any use of pyrophosphatase to relieve inhibition. Based on observations for *in vitro* transcription, pyrophosphatase would be expected to enhance these reactions. Yet, other adenylate-forming enzymes seem to function adequately *in vitro*. For example, nonribosomal peptide synthesis (NRPS) was reconstituted without the addition of pyrophosphatase despite the presence of adenylation domains in selected NRPS enzymes [51]. Additionally, a recently reported NRPS-like enzyme that has an adenylate-forming domain and generates aldehydes from carboxylic acid substrates appears to achieve high yields (in some cases > 90%) without pyrophosphatase addition [52]. Although the reactions catalyzed by this NRPS-like enzyme nearly achieve completion after roughly 24 hours under conditions investigated, it is possible that addition of pyrophosphatase may increase the rate of conversion.

In the case of *in vitro* aldehyde biosynthesis using purified CARs, we can be more certain that pyrophosphatase addition should enhance conversion and allow for higher initial substrate concentrations. Results presented in this study also motivate the use of pyrophosphatase whenever CARs are harnessed for *in vitro* pathways in dilute solution. A few studies published during roughly the past decade have reported attempts towards larger-scale *in vitro* aldehyde synthesis [18] or towards *in vitro* reconstitution of a multi-enzyme pathway featuring CARs [16, 25] without pyrophosphatase addition. As a result, these experiments either suffered from low conversions or were limited to small (< 1 mM) initial substrate concentrations. In such scenarios, and any others in which more data than initial rate measurements is desired, our study strongly suggests that pyrophosphatase should be included in the reaction to avoid early termination.

The history of CAR assays provides an interesting perspective into why the influence of pyrophosphatase on CAR kinetics may have been previously overlooked. When one of the first reported enzymes of the CAR class, CAR from *Neurospora crassa*, was characterized by Gross and Zenk in 1969, the authors formulated the reaction as potentially involving the formation of ADP and inorganic phosphate rather than AMP and PP_i [53]. Thus, they had no rationale to include pyrophosphatase in the original activity assay, which became the standard as homologs were discovered. However, in 1972, Gross demonstrated that the same CAR from *Neurospora crassa* generates an acyl-adenylate intermediate and revised his original formulation [54]. Pyrophosphatase was used in the ATP exchange assay that revealed the acyl-adenylate intermediate, but there was no mention of possible inhibition from PP_i or relief from pyrophosphatase addition. In 1991, when Kato and colleagues reported characterization of a related CAR from *Nocardia asteroides*, the authors assayed activity using the method of Gross and Zenk (i.e., in the absence of pyrophosphatase), although they independently confirmed the presence of an acyl-adenylate intermediate using pyrophosphatase [55]. Use of pyrophosphatase alongside CARs appears to have not been reported since then and never reported in the context of enzyme kinetics or preparative reactions.

The results from this study shed much light on the discrepancy in performance of CARs observed *in vitro* versus *in vivo*. Because pyrophosphatases are abundant in *E. coli* and other organisms, inhibition by pyrophosphate is not expected to occur in an *in vivo* context. This suggests that cell-free aldehyde biosynthetic processes utilizing cellular extract probably would not suffer from low conversions of carboxylic acid substrates. However, introduction of many other cellular components along with pyrophosphatase would decrease the ease of product purification, a supposed advantage of an *in vitro* biosynthetic process. More importantly, cell-free extract could

only be derived from cells that have been engineered to contain decreased endogenous aldehyde reductase activity.

5 Conclusion

Aldehydes are valuable for many purposes where their biosynthesis may be preferred over chemical synthesis, including as flavors and fragrances. In addition, the reactivity of aldehydes allows for numerous potential enzymatic steps downstream if aldehyde biosynthesis can occur robustly. We have demonstrated that Car$_{Ni}$-catalyzed conversion of carboxylic acids to aldehydes ordinarily suffers from low yields *in vitro* but that pyrophosphate hydrolysis enabled by addition of inorganic pyrophosphatase increases yields and improves predictability of reaction kinetics. Given currently limited understanding of microbial aldehyde toxicity and surging commercial interest in aldehyde biosynthesis [56], these results aid in informing potential development of cell-free *in vitro* aldehyde biosynthesis for applications in flavor and related industries.

Acknowledgements

We thank Professor Hadley D. Sikes (Department of Chemical Engineering, MIT) for providing access to an ÄKTApurifier. In addition, we are indebted to Brandon W. Heimer, Joseph B. Lim, and Matt D. McMahon for their assistance with protein purification. This research was supported by the National Science Foundation through the Synthetic Biology Engineering Research Center (SynBERC, Grant No. EEC-0540879) and through a Graduate Research Fellowship to A.M.K.

Figure Legends:

Fig. 1: Addition of inorganic pyrophosphatase from *E. coli* (Ppa_{Ec}) improves *in vitro* conversion of benzoate to benzaldehyde catalyzed by the carboxylic acid reductase from *Nocardia iowensis* (Car_{Ni}). (A) Simplified reaction for Car_{Ni} depicting all required co-factors. (B) Reaction scheme for Ppa_{Ec}. (C) Effect of perturbing ATP, $MgCl_2$, and Ppa_{Ec} concentrations on benzoate and benzaldehyde concentrations from *in vitro* reactions catalyzed by Car_{Ni} at 30 minutes and at 60 minutes. In every case, the rate of conversion dramatically slowed after 30 minutes, underscoring the problem of limited turnover. A two-fold increase in ATP concentration from 6 mM to 12 mM did not improve conversion. A five-fold increase in $MgCl_2$ concentration from 20 mM to 100 mM along with the higher ATP concentration also did not improve conversion. On the other hand, Ppa_{Ec} addition at the original ATP and $MgCl_2$ concentrations substantially enhanced conversion of benzoate to benzaldehyde.

Fig. 2: Effects of perturbing $MgCl_2$ concentration and adding Ppa_{Ec} (224 nM) on a two-enzyme *in vitro* reaction pathway involving Car_{Ni} (224 nM) and a heterologous aldo-keto reductase, $YtbE_{Bs}$ (1422 nM). $YtbE_{Bs}$, which catalyzes the conversion of benzaldehyde into benzyl alcohol, was included to investigate whether the reaction catalyzed by Car_{Ni} would be enhanced by creating a sink for the product and to evaluate the performance of Car_{Ni} in an *in vitro* pathway (benzoate → benzaldehyde → benzyl alcohol). In this case, the objective is to maximum yield of the aldehyde-derived product (benzyl alcohol). Subsequent experiments (Fig. S2) showed that the higher concentration of $MgCl_2$ slightly reduced the activity of the second enzyme.

Fig. 3: Addition of Ppa_{Ec} to *in vitro* reactions containing Car_{Ni} enables greater predictability of reaction progress. (A) Michaelis-Menten kinetic curve displaying specific activity of Car_{Ni} during initial rate measurements at corresponding benzoate concentrations. (B) Comparison of modeling

results with experimental results for longer term conversion of benzoate to benzaldehyde catalyzed by Car$_{Ni}$. Dashed lines represent simulated concentrations, whereas "x" and "o" symbols represented measured concentrations. Left and right panels display measured concentrations in the absence ("x") or presence ("o") of Ppa$_{Ec}$, respectively. Colors corresponding to pathway molecules are consistent with previous data: green = benzoate; yellow = benzaldehyde. Model parameters: $K_{M,\ Car\_Ni\text{-}GBD}$ = 0.35 mM; $k_{cat,\ Car\_Ni\text{-}GBD}$ = 216 min^{-1}. [Car$_{Ni}$] = 224 nM. (C) Michaelis-Menten kinetic curve displaying specific activity of YtbE$_{Bs}$ during initial rate measurements at corresponding benzaldehyde concentrations. (D) Comparison of modeling results with experimental results for a two-enzyme *in vitro* pathway (benzoate → benzaldehyde → benzyl alcohol) containing Car$_{Ni}$ and YtbE$_{Bs}$. The objective is to maximum yield of the aldehyde-derived product (benzyl alcohol). Left and right panels are consistent with (B). Red lines and symbols represent benzyl alcohol. Model parameters: $K_{M,\ YtbE\_Bs\text{-}SH3}$ = 2 mM; $k_{cat,\ YtbE\_Bs\text{-}SH3}$ = 96 min^{-1}. [YtbE$_{Bs}$] = 1422 nM. Error bars omitted in (B) and (D) for clarity; however, deviations between duplicate measurements were less than 5% of average values.

Fig. 4: Effect of Ppa$_{Ec}$ addition on the Car$_{Ni}$-catalyzed conversions of two substrates that result in aldehydes valuable as flavors. χ represents the conversion of substrate C_i ($\chi = C_i/C_{i0}$). Initial substrate concentrations were 5 mM, a five-fold increase compared to previous experiments. Concentrations of ATP and NADPH were each maintained at 6 mM. In this case, reactions containing Ppa$_{Ec}$ may not have attained full conversion within 120 minutes due to limiting co-factor pools towards the end of the reactions. In spite of that, final conversion roughly doubled for both substrates in the presence of Ppa$_{Ec}$.

Figures:

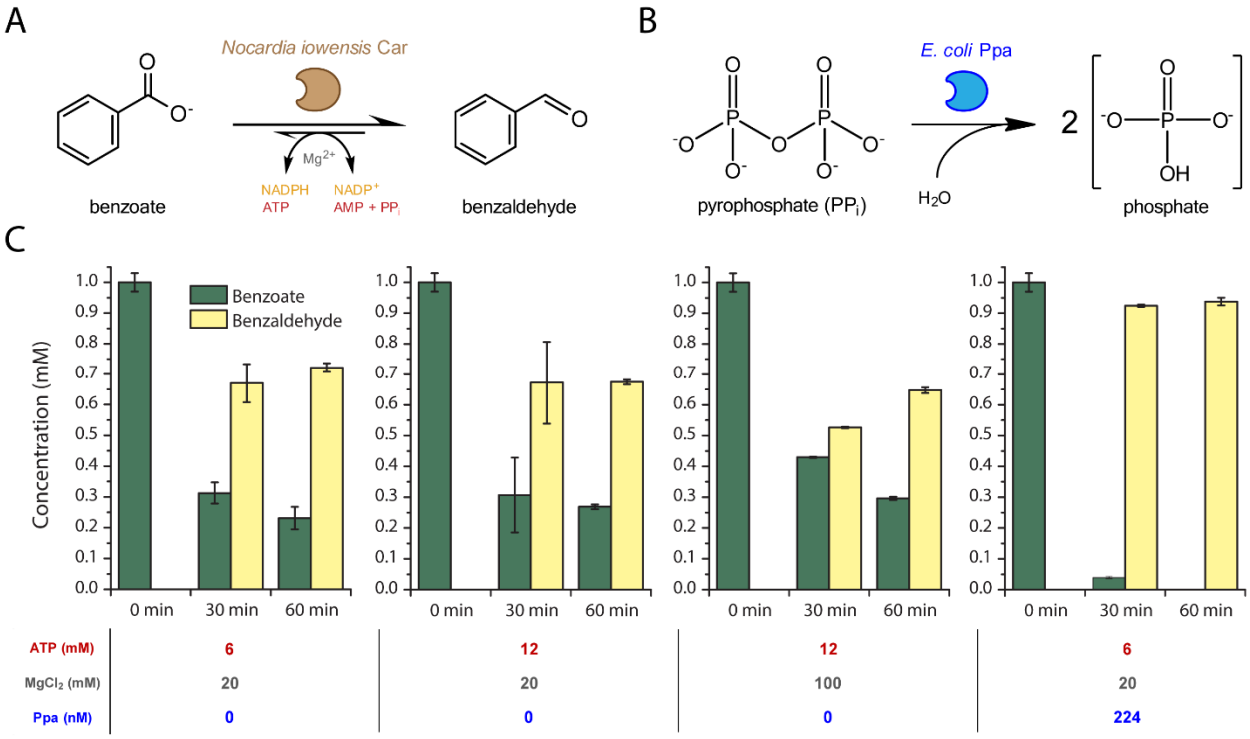

Fig. 1.

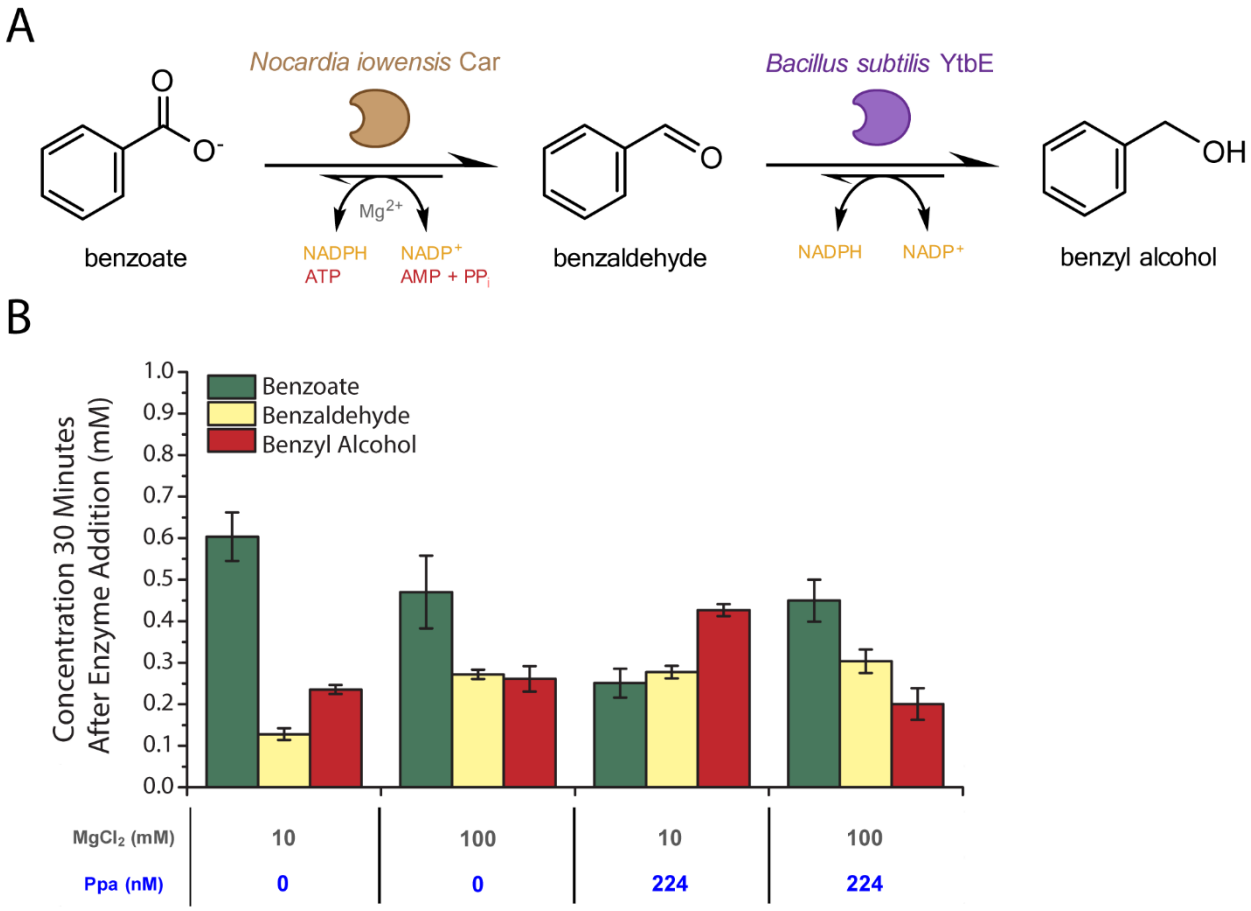
A
Nocardia iowensis Car
Bacillus subtilis YtbE
benzoate
NADPH
ATP
NADP+
AMP + PPi
benzaldehyde
NADPH
NADP+
benzyl alcohol
B
Concentration 30 Minutes After Enzyme Addition (mM)
Benzoate
Benzaldehyde
Benzyl Alcohol
MgCl2 (mM)
Ppa (nM)
10
0
100
0
10
224
100
224

Fig. 2.

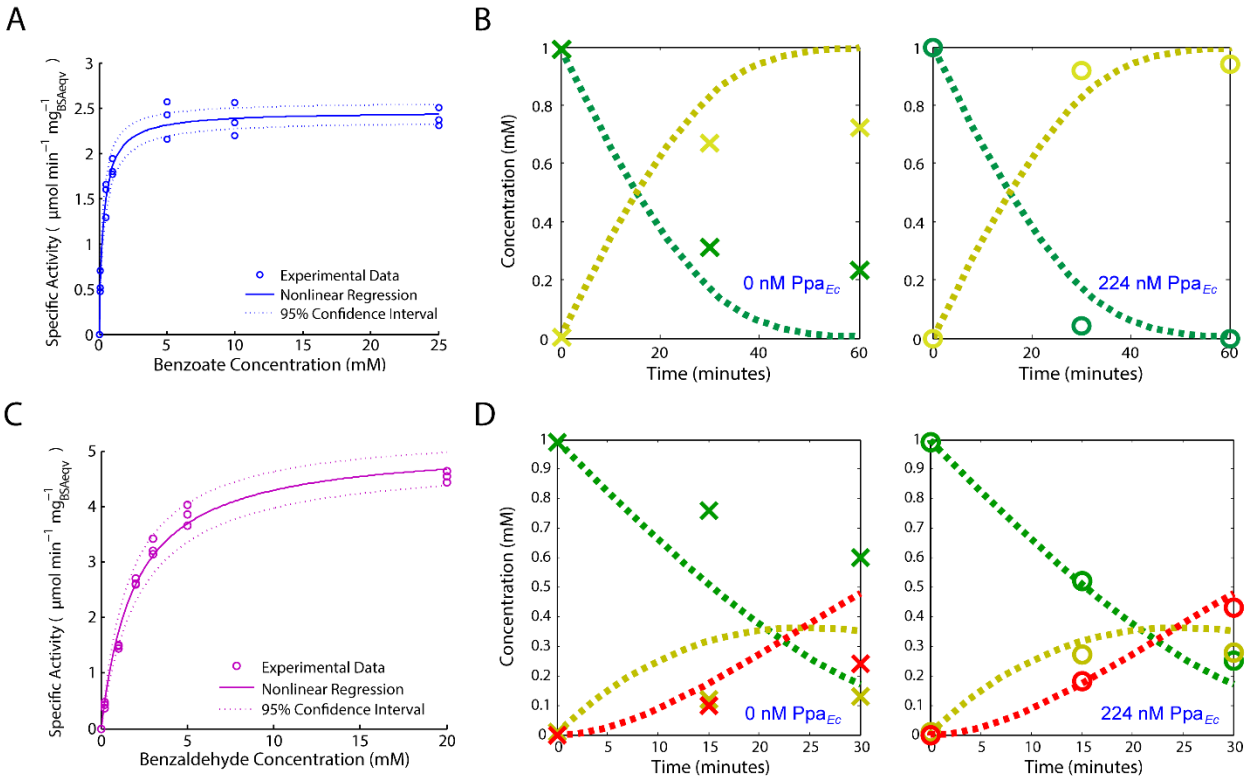
A
B
C
D
Specific Activity (µmol min−1 mgBSAeqv−1)
Benzoate Concentration (mM)
Experimental Data
Nonlinear Regression
95% Confidence Interval
Concentration (mM)
Time (minutes)
0 nM PpaEc
224 nM PpaEc
Benzaldehyde Concentration (mM)

Fig. 3.

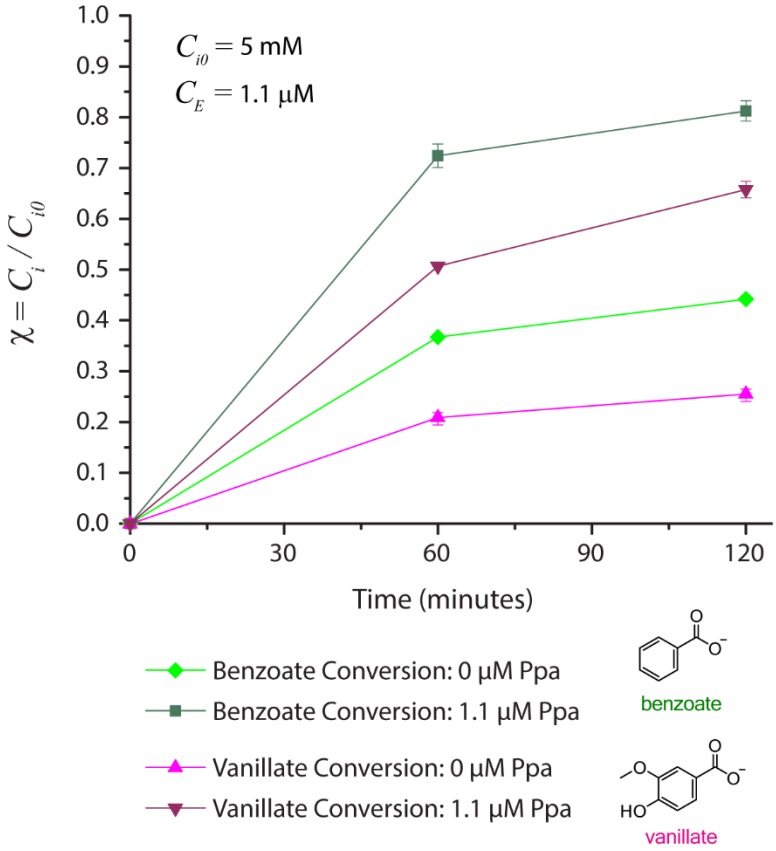
$C_{i0} = 5$ mM
$C_E = 1.1$ μM
$\chi = C_i / C_{i0}$
1.0
0.9
0.8
0.7
0.6
0.5
0.4
0.3
0.2
0.1
0.0
0
30
60
90
120
Time (minutes)
Benzoate Conversion: 0 μM Ppa
Benzoate Conversion: 1.1 μM Ppa
Vanillate Conversion: 0 μM Ppa
Vanillate Conversion: 1.1 μM Ppa
benzoate
vanillate

Fig. 4.

References:

[1] A. Lomascolo, C. Stentelaire, M. Asther, L. Lesage-Meessen, Basidiomycetes as new biotechnological tools to generate natural aromatic flavours for the food industry, Trends in biotechnology, 17 (1999) 282-289.
[2] U. Krings, R.G. Berger, Biotechnological production of flavours and fragrances, Applied Microbiology and Biotechnology, 49:1 (1998) 1-8.
[3] G. Feron, Y. Wache, 1.16 Microbial Biotechnology of Food Flavor Production, in: A. Pometto, K. Shetty, G. Paliyath, R. Levin (Eds.) Food Biotechnology, Second Edition, CRC Press, Boca Raton, FL, 2006, pp. 407-442.
[4] K.-G. Fahlbusch, F.-J. Hammerschmidt, J. Panten, W. Pickenhagen, D. Schatkowski, K. Bauer, D. Garbe, H. Surburg, Flavors and Fragrances, Ullmann's Encyclopedia of Industrial Chemistry, Wiley-VCH Verlag GmbH & Co. KGaA2000.
[5] S. Hagedorn, B. Kaphammer, Microbial Biocatalysis in the Generation of Flavor and Fragrance Chemicals, Annual Review of Microbiology, 48 (1994) 773-800.
[6] P.A. Tarantilis, M.G. Polissiou, Isolation and Identification of the Aroma Components from Saffron (Crocus sativus), Journal of Agricultural and Food Chemistry, 45 (1997) 459-462.
[7] N.J. Walton, M.J. Mayer, A. Narbad, Vanillin, Phytochemistry, 63 (2003) 505-515.
[8] G.A. Burdock, Fenaroli's Handbook of Flavor Ingredients, CRC Press, Boca Raton, Florida, 2005.
[9] C.E. Hodgman, M.C. Jewett, Cell-free synthetic biology: Thinking outside the cell, Metabolic engineering, 14 (2012) 261-269.
[10] J.R. Swartz, Transforming biochemical engineering with cell-free biology, AICHE Journal, 58 (2012) 5-13.
[11] A.M. Kunjapur, K.L.J. Prather, Microbial Engineering for Aldehyde Synthesis, Applied and Environmental Microbiology, 81 (2015) 1892-1901.
[12] A.M. Kunjapur, Y. Tarasova, K.L.J. Prather, Synthesis and Accumulation of Aromatic Aldehydes in an Engineered Strain of Escherichia coli, J. Am. Chem. Soc., 136 (2014) 11644-11654.
[13] J. Zaldivar, A. Martinez, L.O. Ingram, Effect of selected aldehydes on the growth and fermentation of ethanologenic Escherichia coli, Biotechnology and Bioengineering, 65 (1999) 24-33.
[14] C. Huang, H. Wu, Q.-p. Liu, Y.-y. Li, M.-h. Zong, Effects of Aldehydes on the Growth and Lipid Accumulation of Oleaginous Yeast Trichosporon fermentans, Journal of Agricultural and Food Chemistry, 59 (2011) 4606-4613.
[15] L. Wang, P. Tang, X. Fan, Q. Yuan, Effect of selected aldehydes found in the corncob hemicellulose hydrolysate on the growth and xylitol fermentation of Candida tropicalis, Biotechnology Progress, 29 (2013) 1181-1189.
[16] K. Napora-Wijata, G.A. Strohmeier, M. Winkler, Biocatalytic reduction of carboxylic acids, Biotechnology Journal, 9 (2014) 822-843.
[17] T. Li, J.P. Rosazza, Purification, characterization, and properties of an aryl aldehyde oxidoreductase from Nocardia sp. strain NRRL 5646, The Journal of Bacteriology, 179 (1997) 3482-3487.
[18] A. He, T. Li, L. Daniels, I. Fotheringham, J.P.N. Rosazza, Nocardia sp. Carboxylic Acid Reductase: Cloning, Expression, and Characterization of a New Aldehyde Oxidoreductase Family, Applied and Environmental Microbiology, 70 (2004) 1874-1881.
[19] P. Venkitasubramanian, L. Daniels, J.P.N. Rosazza, Reduction of Carboxylic Acids by Nocardia Aldehyde Oxidoreductase Requires a Phosphopantetheinylated Enzyme, Journal of Biological Chemistry, 282 (2007) 478-485.
[20] P. Venkitasubramanian, L. Daniels, S. Das, A.S. Lamm, J.P.N. Rosazza, Aldehyde oxidoreductase as a biocatalyst: Reductions of vanillic acid, Enzyme and Microbial Technology, 42 (2008) 130-137.

[21] E.H. Hansen, B.L. Møller, G.R. Kock, C.M. Bünner, C. Kristensen, O.R. Jensen, F.T. Okkels, C.E. Olsen, M.S. Motawia, J. Hansen, De Novo Biosynthesis of Vanillin in Fission Yeast (Schizosaccharomyces pombe) and Baker's Yeast (Saccharomyces cerevisiae), Applied and Environmental Microbiology, 75 (2009) 2765-2774.
[22] M.J. Sheppard, A.M. Kunjapur, S.J. Wenck, K.L.J. Prather, Retro-biosynthetic screening of a modular pathway design achieves selective route for microbial synthesis of 4-methyl-pentanol, Nat Commun, 5 (2014) 5031.
[23] K. Li, J.W. Frost, Synthesis of Vanillin from Glucose, Journal of the American Chemical Society, 120 (1998) 10545-10546.
[24] J. Shin, V. Noireaux, An E. coli Cell-Free Expression Toolbox: Application to Synthetic Gene Circuits and Artificial Cells, ACS Synthetic Biology, 1 (2012) 29-41.
[25] M.K. Akhtar, N.J. Turner, P.R. Jones, Carboxylic acid reductase is a versatile enzyme for the conversion of fatty acids into fuels and chemical commodities, Proc. Natl. Acad. Sci. U.S.A., 110 (2013) 87-92.
[26] J.E. Dueber, G.C. Wu, G.R. Malmirchegini, T.S. Moon, C.J. Petzold, A.V. Ullal, K.L.J. Prather, J.D. Keasling, Synthetic protein scaffolds provide modular control over metabolic flux, Nat Biotech, 27 (2009) 753-759.
[27] M.M. Bradford, A rapid and sensitive method for the quantitation of microgram quantities of protein utilizing the principle of protein-dye binding, Analytical Biochemistry, 72 (1976) 248-254.
[28] J.W. Ogilvie, S.C. Whitaker, Reaction of tris with aldehydes: Effect of tris on reactions catalyzed by homoserine dehydrogenase and glyceraldehyde-3-phosphate dehydrogenase, Biochimica et Biophysica Acta (BBA) - Enzymology, 445 (1976) 525-536.
[29] W.A. Bubb, H.A. Berthon, P.W. Kuchel, Tris Buffer Reactivity with Low-Molecular-Weight Aldehydes: NMR Characterization of the Reactions of Glyceraldehyde-3-Phosphate, Bioorganic Chemistry, 23 (1995) 119-130.
[30] S. Schmelz, J.H. Naismith, Adenylate-forming enzymes, Current Opinion in Structural Biology, 19 (2009) 666-671.
[31] Y. Mori, K. Nagamine, N. Tomita, T. Notomi, Detection of Loop-Mediated Isothermal Amplification Reaction by Turbidity Derived from Magnesium Pyrophosphate Formation, Biochemical and biophysical research communications, 289 (2001) 150-154.
[32] J. Lei, Y.-F. Zhou, L.-F. Li, X.-D. Su, Structural and biochemical analyses of YvgN and YtbE from Bacillus subtilis, Protein Science, 18 (2009) 1792-1800.
[33] Y. Ni, C.-X. Li, H.-M. Ma, J. Zhang, J.-H. Xu, Biocatalytic properties of a recombinant aldo-keto reductase with broad substrate spectrum and excellent stereoselectivity, Applied Microbiology and Biotechnology, 89 (2011) 1111-1118.
[34] A.A. Baykov, A.S. Shestakov, V.N. Kasho, A.V. Vener, A.H. Ivanov, Kinetics and thermodynamics of catalysis by the inorganic pyrophosphatase of Escherichia coli in both directions, European Journal of Biochemistry, 194 (1990) 879-887.
[35] A.A. Baykov, T. Hyytia, S.E. Volk, V.N. Kasho, A.V. Vener, A. Goldman, R. Lahti, B.S. Cooperman, Catalysis by Escherichia coli Inorganic Pyrophosphatase: pH and Mg2+ Dependence, Biochemistry, 35 (1996) 4655-4661.
[36] L. Peller, In vitro RNA synthesis should be coupled to pyrophosphate hydrolysis, Biochemical and Biophysical Research Communications, 63 (1975) 912-916.
[37] J.A. Kern, R.H. Davis, Application of Solution Equilibrium Analysis to *in Vitro* RNA Transcription, Biotechnology progress, 13 (1997) 747-756.
[38] S. Akama, M. Yamamura, T. Kigawa, A Multiphysics Model of In Vitro Transcription Coupling Enzymatic Reaction and Precipitation Formation, Biophysical journal, 102 (2012) 221-230.

[39] S. Billerbeck, J. Härle, S. Panke, The good of two worlds: increasing complexity in cell-free systems, Current Opinion in Biotechnology, 24 (2013) 1037-1043.
[40] A. Meyer, R. Pellaux, S. Panke, Bioengineering novel in vitro metabolic pathways using synthetic biology, Current Opinion in Microbiology, 10 (2007) 246-253.
[41] J. Josse, Constitutive Inorganic Pyrophosphatase of Escherichia coli : I. PURIFICATION AND CATALYTIC PROPERTIES, Journal of Biological Chemistry, 241 (1966) 1938-1947.
[42] J. Josse, R.A.D. With an appendix by, Constitutive Inorganic Pyrophosphatase of Escherichia coli : II. NATURE AND BINDING OF ACTIVE SUBSTRATE AND THE ROLE OF MAGNESIUM, Journal of Biological Chemistry, 241 (1966) 1948-1954.
[43] S.C.K. Wong, D.C. Hall, J. Josse, Constitutive Inorganic Pyrophosphatase of Escherichia coli : III. MOLECULAR WEIGHT AND PHYSICAL PROPERTIES OF THE ENZYME AND ITS SUBUNITS, Journal of Biological Chemistry, 245 (1970) 4335-4341.
[44] P.M. Burton, D.C. Hall, J. Josse, Constitutive Inorganic Pyrophosphatase of Escherichia coli : IV. CHEMICAL STUDIES OF PROTEIN STRUCTURE, Journal of Biological Chemistry, 245 (1970) 4346-4352.
[45] J. Chen, A. Brevet, M. Fromant, F. Lévêque, J.M. Schmitter, S. Blanquet, P. Plateau, Pyrophosphatase is essential for growth of Escherichia coli, Journal of Bacteriology, 172 (1990) 5686-5689.
[46] R.H. Upson, R.P. Haugland, M.N. Malekzadeh, R.P. Haugland, A Spectrophotometric Method to Measure Enzymatic Activity in Reactions That Generate Inorganic Pyrophosphate, Analytical Biochemistry, 243 (1996) 41-45.
[47] P.R. Cunningham, J. Ofengand, Use of inorganic pyrophosphatase to improve the yield of in vitro transcription reactions catalyzed by T7 RNA polymerase, Eaton, Natick, MA, ETATS-UNIS, 1990.
[48] I.D. Pokrovskaya, V.V. Gurevich, In Vitro Transcription: Preparative RNA Yields in Analytical Scale Reactions, Analytical Biochemistry, 220 (1994) 420-423.
[49] A. Rodriguez, E. Meighen, Fatty acyl-AMP as an intermediate in fatty acid reduction to aldehyde in luminescent bacteria, Journal of Biological Chemistry, 260 (1985) 771-774.
[50] M. Deluca, W. McElroy, [1] Purification and properties of firefly luciferase, Methods in Enzymology, 57 (1978) 3-15.
[51] E.S. Sattely, M.A. Fischbach, C.T. Walsh, Total biosynthesis: in vitro reconstitution of polyketide and nonribosomal peptide pathways, Natural Product Reports, 25 (2008) 757-793.
[52] M. Wang, H. Zhao, Characterization and Engineering of the Adenylation Domain of a NRPS-Like Protein: A Potential Biocatalyst for Aldehyde Generation, ACS Catalysis, 4 (2014) 1219-1225.
[53] G.G. Gross, M.H. Zenk, Reduktion aromatischer Säuren zu Aldehyden und Alkoholen im zellfreien System, European Journal of Biochemistry, 8 (1969) 413-419.
[54] G.G. Gross, Formation and Reduction of Intermediate Acyladenylate by Aryl-Aldehyde, European Journal of Biochemistry, 31 (1972) 585-592.
[55] N. Kato, E.-H. Joung, H.-C. Yang, M. Masuda, M. Shimao, H. Yanase, Purification and Characterization of Aromatic Acid Reductase from Nocardia asteroides JCM 3016, Agricultural and Biological Chemistry, 55 (1991) 757-762.
[56] E.C. Hayden, Synthetic-biology firms shift focus, *Nature*, 505 (2014) 598.

Graphical Abstract: